

Transport of excitations in disordered systems: Self-consistent density resummation

Johan Nieuwoudt and Shaul Mukamel

Department of Chemistry, University of Rochester, Rochester, New York 14627

(Received 16 February 1984; revised manuscript received 14 May 1984)

New self-consistent equations for the transport of excitations in disordered systems are derived based on a resummation procedure of the density expansion. Both local-time [partial-time-ordering prescription (POP)] and convolution-type [chronological-time-ordering prescription] equations are explored. Application is made to a system consisting of a random mixture of donors and traps with a general type of transfer rate $W(r)$. We calculate the probability of remaining in the original site $G_0(t)$ as well as the second moment of the distribution of excitations $\langle r^2(t) \rangle$. The POP equations reduce to the exact Forster solution for $G_0(t)$ in the case of traps only. We analyze the long-time behavior of $G_0(t)$ and its dependence on $W(r)$. We find a percolation-type transition when $W(r)$ has a cutoff [i.e., $W(r)=0$ for $r > r_0$] but in all other cases the system is diffusive at long times [$G_0(t)$ vanishes and $\langle r^2(t) \rangle$ diverges linearly in time].

I. INTRODUCTION

The dynamics of excitations or particles in disordered systems have been the subject of numerous theoretical and experimental studies.¹⁻⁹ Recent theoretical studies include computer simulations,^{3,10-13} cluster expansions,¹⁴ effective-medium approximations,¹⁵⁻¹⁷ Green's-function, ¹⁸⁻²⁴ and renormalization-group techniques.^{25,26}

Haan and Zwanzig¹⁴ (HZ) had used a low-density (cluster) expansion towards the calculation of the transfer of excitations between donors with Forster (r^{-6}) transition rates. A quantitative understanding of the long-time (and low-frequency) behavior of these systems requires, however, the resummation of the cluster expansions to infinite order in density. Such a resummation is particularly important in model systems which exhibit a critical behavior (e.g., percolation). Low-order density expansions fail to reproduce the critical behavior of such systems. Gouchanour, Andersen, and Fayer¹⁸ (GAF) and Loring, Andersen, and Fayer¹⁹ (LAF) had developed a diagrammatic self-consistent equation (SCE) which provides a partial summation of diagrams and applies also to high densities. Both HZ and GAF have used the conventional reduced equation of motion (REM) with memory (i.e., nonlocal in time) within the chronological-time-ordering prescription (COP). An alternative local-time formalism has been developed in recent years. It is based on a partial-time-ordering prescription (POP).²⁷ Applications of the local-time formalism were made to nonlinear optics, and spectral line shapes,^{27(b)} reduced theory of scattering,^{27(c)} mode-coupling problems,^{27(d)} and intramolecular line broadening in anharmonic molecules.²⁸ Specific applications to the electrical conductivity and transfer of excitations in disordered systems were recently made.²⁹

Both the COP and POP formalisms are in principle exact, provided the necessary kernels are evaluated rigorously. Also, in the Markovian (diffusive) limit when the second moment of the distribution of excitations grows linearly with time, they are both identical. However, once

approximations are made and partial summations carried out in non-Markovian situations, then they have drastically different predictions. It should be noted that the POP formulation is frequently used in the studies of stochastic processes³⁰ whereas many-body theory and nonequilibrium statistical mechanics are usually formulated within the COP scheme.³¹

We feel that the POP scheme may be advantageous for the treatment of the dynamics of excitations in disordered systems. If we consider a system consisting of one donor and M traps (the Forster problem¹), then the exact probability of the excitation to remain on the initial donor at time t is [see Eq. (12)]

$$G_0(t) = \exp \left[- \int_0^t d\tau (t-\tau) \tilde{F}(\tau) \right]. \quad (1a)$$

$\tilde{F}(\tau)$ is a function of time and is linear in the concentration of traps c_T , i.e.,

$$\tilde{F}(\tau) = c_T F^{(1)}(\tau). \quad (1b)$$

The kernel in the POP equation (1a) is therefore rigorously first order in c_T . Within the COP formulation, on the other hand, we write [see Eq. (40)]

$$G_0(t) = \int_{-\infty}^{\infty} d\epsilon \exp(i\epsilon t) \frac{1}{i\epsilon + \tilde{H}(c_T, \epsilon)}, \quad (2a)$$

where

$$\tilde{H}(c_T, \epsilon) = \sum_{n=1}^{\infty} c_T^n \tilde{H}^{(n)}(\epsilon). \quad (2b)$$

The COP kernel \tilde{H} , even in this simple case, is an infinite-order expansion in c_T and is therefore much more complicated than $\tilde{F}(\tau)$. It seems therefore natural to develop a self-consistent equation using the POP scheme which will hold for an arbitrary mixture of donors and traps and will reduce to Eq. (1a) when the donor concentration $c_D \rightarrow 0$. In this paper we develop a systematic SCE within the local-time formulation. We further analyze the universality classes of the long-time behavior

of disordered systems according to the functional form of the transfer rate $W(r)$. We find that there is no qualitative difference between long-range (r^{-m}) and short-range [$\exp(-r)$] transfer rates. However, we do find a difference when $W(r)$ contains an upper cutoff. We further compare systematically the predictions of the local-time and the convolution types of SCE.

The plan of the paper is as follows. In Sec. II the basic equations for the dynamics of excitations are given, and POP forms for $G_0(t)$ and the total Green's function $G(\vec{k}, t)$ are derived. In Sec. III the self-consistent equation [Eqs. (37)] for $G_0(t)$ is developed for a general transfer rate $W(r)$. A resummed expression for the second moment $\langle r^2(t) \rangle$ is also given in terms of $G_0(t)$ [Eq. (39)]. Section IV contains a parallel derivation of the corresponding COP equations. Solutions of the SCE for finite and infinite ranged $W(r)$ are presented in Sec. V within the lowest order (two-body) approximation. Section VI contains a solution of the COP SCE within the three-body approximation. Finally the results are summarized and discussed in Sec. VII.

II. THE BASIC FORMALISM

We consider a system of N "donor" particles and M "trap" particles distributed randomly in a volume V . We denote the donor and trap particle densities by c_D and c_T , respectively, where $c_D \equiv N/V$ and $c_T \equiv M/V$. Both c_D and c_T remain finite in the thermodynamic limit where $M, N, V \rightarrow \infty$.

The probability of finding an excitation (e.g., electronic excitation, an electron, etc.) on a donor is denoted by $P_i(\vec{R}, t)$ for $1 \leq i \leq N$ and of finding it on a trap is denoted by $P_j(\vec{R}, t)$ for $N+1 \leq j \leq N+M$. $\vec{R} = (\vec{r}_1, \vec{r}_2, \dots, \vec{r}_{N+M})$ denotes a specific configuration of the donors and traps. We assume that the evolution of these probabilities is described by the following master equation:³²

$$\frac{d}{dt} P_i(t) = \sum_{j=1}^N w_{ij} (P_j - P_i) - \sum_{j=N+1}^{N+M} w_{ji} P_i, \quad i < N \quad (3a)$$

$$\frac{d}{dt} P_j(t) = \sum_{i=1}^N w_{ji} P_i, \quad N+1 \leq j \leq N+M. \quad (3b)$$

w_{ij} is the rate at which the excitation hops among the donors and to a trap. We shall assume that w_{ij} is isotropic and depends only on $|\vec{r}_{ij}|$, and that $w_{ii} = 0$.

The master equation (3) can be written in matrix notation as

$$\frac{d}{dt} \vec{P}(t) = \underline{W} \cdot \vec{P}(t), \quad (4)$$

where \underline{W} is given by

$$W_{ij} = \begin{cases} w_{ij} - \delta_{ij} \left[\sum_{k=1}^{N+M} w_{kj} \right], & k, j < N+1 \\ w_{ij}, & N+M > i > N+1, j < N+1 \\ 0, & j \geq N+1. \end{cases} \quad (5)$$

Equation (4) has the formal solution

$$\vec{P}(t) = \exp(\underline{W}t) \vec{P}(0). \quad (6)$$

Following Haan and Zwanzig¹⁴ we define an average density of excitations at point \vec{r} by

$$\langle P(\vec{r}, t) \rangle \equiv \left\langle \sum_{j=1}^{N+M} \delta(\vec{r} - \vec{r}_j) P_j(\vec{R}, t) \right\rangle, \quad (7a)$$

where the angular brackets denote averaging over all possible random configurations of the donors and traps, i.e.,

$$\langle \dots \rangle \equiv V^{-N-M} \int d\vec{r}_1 \dots d\vec{r}_{N+M} \dots \quad (7b)$$

Using a Green's function to represent $\langle P(\vec{r}, t) \rangle$, Eq. (7a) is written as

$$\langle P(\vec{r}, t) \rangle = \int d\vec{r}' G(\vec{r} - \vec{r}', t) \langle P(\vec{r}', 0) \rangle, \quad (8a)$$

where

$$G(\vec{r} - \vec{r}', t) \equiv \frac{V}{N} \sum_{i=1}^{N+M} \sum_{j=1}^N \langle \delta(\vec{r}_i - \vec{r}') \exp(\underline{W}t)_{ij} \times \delta(\vec{r} - \vec{r}_j) \rangle, \quad (8b)$$

and where it is assumed that the excitation is initially on a donor. Since the transfer rates w_{ij} depend only on the relative coordinates of particles i and j , the averaged system is translationally invariant and G depends only on $\vec{r} - \vec{r}'$. When the double sum and the averaging process in Eq. (8) are carried out, only three distinct terms remain. They are¹⁴

$$G(\vec{r} - \vec{r}', t) = \delta(\vec{r} - \vec{r}') \langle \exp(\underline{W}t)_{11} \rangle + (N-1) \langle \delta(\vec{r} - \vec{r}' - \vec{r}_{12}) \exp(\underline{W}t)_{21} \rangle + M \langle \delta(\vec{r} - \vec{r}' - \vec{r}_{N+1,1}) \exp(\underline{W}t)_{N+1,1} \rangle. \quad (9)$$

In this paper we shall be interested in calculating the total Green's function, G , as well as the probability $G_0(t)$ for the excitation to remain on the initially excited donor site, i.e., the first term on the right-hand side (rhs) of Eq. (9)

$$G_0(t) \equiv \langle \exp(\underline{W}t)_{11} \rangle. \quad (10)$$

The remaining two terms in the rhs of Eq. (9) give the distribution of the excitation among the other donors and traps, respectively, at time t . They may be calculated in a similar way and will not be discussed here. The calculation of $G_0(t)$ will be performed by starting with the following *exact* reduced equation of motion:²⁹

$$\frac{dG_0(t)}{dt} = - \int_0^t d\tau \tilde{F}(\tau) G_0(t), \quad (11)$$

whose solution is

$$G_0(t) = \exp \left[- \int_0^t d\tau (t - \tau) \tilde{F}(\tau) \right]. \quad (12)$$

The kernel $\tilde{F}(\tau)$ is given by

$$\tilde{F}(\tau) = - \frac{d^2}{d\tau^2} \ln \langle \exp(\underline{W}\tau)_{11} \rangle - \langle W_{11} \rangle \delta(\tau). \quad (13)$$

Similarly the total Green's function satisfies the following POP equation:²⁹

$$\frac{dG(\vec{k},t)}{dt} = - \left[\int_0^t d\tau k^2 D(k,\tau) \right] G(\vec{k},t), \quad (14)$$

whose solution is

$$G(\vec{k},t) = \exp \left[- \int_0^t d\tau (t-\tau) k^2 D(\vec{k},\tau) \right]. \quad (15)$$

Here $G(\vec{k},t)$ is the spatial Fourier transform of $G(\vec{r},t)$, i.e.,

$$G(\vec{k},t) = \int d\vec{r} \exp(i\vec{k} \cdot \vec{r}) G(\vec{r},t). \quad (16)$$

The generalized diffusion coefficient $D(\vec{k},t)$ is related to \underline{W} by an equation similar to Eq. (13),

$$k^2 D(\vec{k},t) = - \frac{d^2}{dt^2} \ln G(\vec{k},t) - \delta(t) \frac{d}{dt} \ln G(\vec{k},t) \Big|_{t=0}. \quad (17)$$

The factor k^2 in the definition of D arises from conservation of probability [$G(k=0,t)=1$]. Linear terms in \vec{k} vanish due to spatial isotropy. Equation (17) seems at first glance like a trivial identity since when substituted in (15) it will result in $G(\vec{k},t)=G(\vec{k},t)$. However it should be understood as follows: Using the definition of G , we can construct a diagrammatic series for the calculation of $D(\vec{k},t)$. This could be by perturbation theory, a density expansion, etc. By truncating or approximating the series we obtain an approximation for D or G . Although an exact calculation of D is equivalent to an exact calculation of G , once approximations are made, it is usually much better to make them on D and then calculate G via Eq. (15). This corresponds to a partial summation of the diagrammatic series for G . The same argument holds also for Eqs. (12) and (13) whereby $\tilde{F}(\tau)$ is a convenient means for resummation of expansions for $G_0(t)$. The REM [Eqs. (11) and (14)] are time-local differential equations and differ from the more common integro-differential equations with memory. The name POP (partial-time-ordering prescription) implies that when the kernels $\tilde{F}(t)$ and $D(\vec{k},t)$ are expanded perturbatively, the various terms will not be completely time ordered. This is in contrast to the more conventional (convolution) formulation which corresponds to a chronological ordering prescription COP (see Sec. IV).²⁷

The mean-square displacement of an excitation is given by

$$\langle r^2(t) \rangle = \int d\vec{r} \vec{r}^2(t) G(\vec{r},t), \quad (18)$$

where it is assumed that the excitation is initially at position $\vec{r}=\vec{0}$. Using Eq. (15) one finds that (in d dimensions)

$$\langle r^2(\epsilon) \rangle = \frac{2d}{\epsilon^2} D(0,\epsilon), \quad (19)$$

where ϵ is the Laplace transform variable conjugate to t , i.e., for any quantity χ :

$$\chi(\epsilon) \equiv \int_0^\infty \chi(t) \exp(-\epsilon t) dt \quad (20a)$$

and

$$\chi(t) = \frac{1}{2\pi} \int_{-\infty}^\infty d\epsilon \exp(i\epsilon t) \chi(i\epsilon). \quad (20b)$$

A simple approximate relation between G_0 and $\langle r^2(t) \rangle$ may be obtained as follows. If we evaluate $G(\vec{k},t)$ in the long-wavelength ($k \rightarrow 0$) limit by setting $D(\vec{k},t) \cong D(0,t)$ then Eq. (15) results in

$$G(k,t) = \exp \left[- \frac{k^2}{2d} \langle r^2(t) \rangle \right], \quad (21)$$

where $d=1,2,3$ is the spatial dimensionality of the system. A relation between $\langle r^2(t) \rangle$ and $G_0(t)$ is established by using Eqs. (9) and (10), whence

$$G(\vec{r}-\vec{r}' \rightarrow \vec{0},t) = \delta(\vec{r}-\vec{r}') G_0(t) \quad (22)$$

or by integrating over some coarse-grained volume element in d dimensions per particle (V_d):

$$G_0(t) \cong V_d G(\vec{r}=\vec{0},t) = V_d \int d\vec{k} G(\vec{k},t). \quad (23)$$

Equations (21) and (23) then result in

$$G_0(t) = \frac{1}{2} V_d \Gamma \left[\frac{d}{2} \right] \left\langle \frac{1}{2d} r^2(t) \right\rangle^{-2/d}, \quad (24)$$

where Γ denotes the gamma function. A result similar to Eq. (24) has been obtained in one dimension using scaling arguments,⁹ and later extended to d dimensions.^{22,29}

In the next section we shall derive a self-consistent equation for $G_0(t)$. Making use of Eq. (24) we can then get an approximate expression for $\langle r^2(t) \rangle$ and $G(\vec{k},t)$. A different type of relation between $G_0(t)$ and $G(\vec{k},t)$ is discussed in the next section [Eq. (39)].

III. THE POP SELF-CONSISTENT EQUATION

In this section we develop a self-consistent equation (SCE) for $G_0(t)$. This is done in two stages: First, a low-density "naive" expansion is obtained using the cluster-expansion technique of HZ.¹⁴ This expansion is then extended to higher densities using a resummation procedure which results in a SCE for $G_0(t)$. The SCE solutions are valid at short and long times and enable us to find the low-frequency behavior of the excitation transport processes, i.e., diffusion and electrical conductivity. We start with the HZ cluster expansion of $G_0(t)$, i.e.,

$$G_0(t) = 1 + c_D S^{(1,0)}(t) + c_T S^{(0,1)}(t) + c_D^2 S^{(2,0)}(t) + c_T^2 S^{(0,2)}(t) + c_D c_T S^{(1,1)}(t) + \dots \quad (25)$$

The coefficients $S^{(m,n)}$ are density independent. All the coefficients for which $m+n=p$ are obtained by considering clusters of $p+1$ bodies. The two-body coefficients $S^{(1,0)}$ and $S^{(0,1)}$ are

$$S^{(0,1)}(t) = - \int d\vec{r} \{ 1 - \exp[W(\vec{r})t] \} \quad (26)$$

and

$$S^{(1,0)}(t) = - \frac{1}{2} \int d\vec{r} \{ 1 - \exp[2W(\vec{r})t] \}. \quad (27)$$

Explicit expressions for the three-body terms $S^{(2,0)}$, $S^{(0,2)}$, and $S^{(1,1)}$ are given in Appendix A.

As already stated in the Introduction, for the case of traps only ($c_D=0$), Forster developed the exact solution for G_0 . We shall denote it by G_T . To make use of this exact solution, we extract it from G_0 , writing

$$G_0(t) \equiv G_T(t)G_D(t), \quad (28)$$

where

$$G_T(t) \equiv \exp[c_T S^{(0,1)}(t)]. \quad (29)$$

By definition G_T depends on c_T only, whereas G_D depends on c_D and c_T . Equation (28) is simply the definition of G_D . The density expansion of $G_D(t)$ is easily obtained by comparing Eqs. (25), (28), and (29), resulting in

$$G_D(t) = 1 + c_D S^{(1,0)} + c_D c_T (S^{(1,1)} - S^{(1,0)} S^{(0,1)}) + c_D^2 S^{(2,0)} + \dots \quad (30)$$

We are now in a position to derive a resummed expression for $G_D(t)$. It should be emphasized that the low-density expansion [Eq. (30)] is the only microscopic input required for our resummation procedure. We start by using the form Eq. (11) for $G_0(t)$ and write

$$G_D(t) = \exp \left[- \int_0^t d\tau (t-\tau) \tilde{F}(c_D, c_T, \tau) \right]. \quad (31)$$

We next introduce a new function \hat{F} which is related to the Laplace transform of \tilde{F} , i.e.,

$$\hat{F}(1/\epsilon) \equiv \int_0^\infty d\tau \exp(-\epsilon\tau) \tilde{F}(\tau), \quad (32a)$$

then

$$G_D(t) = \exp \left[\frac{1}{2\pi} \int_{-\infty}^\infty \frac{d\epsilon}{\epsilon^2} \exp(i\epsilon t) \hat{F}(c_D, c_T, 1/i\epsilon) \right]. \quad (32b)$$

\hat{F} is assumed to have a naive density expansion similar to Eq. (25), i.e.,

$$\hat{F}(c_D, c_T, 1/\epsilon) = \sum_{n,m=0}^\infty c_D^n c_T^m \hat{F}^{(n,m)}(1/\epsilon), \quad (33a)$$

where

$$\hat{F}^{(0,0)} = 0. \quad (33b)$$

The coefficients $\hat{F}^{(n,m)}$ are determined by substituting Eq. (33a), and the expansion for G_D [Eq. (30)] into Eq. (32) and comparing equal powers of the density. The results to $O(c^2)$ are given in Appendix B.

The resummation of the series [Eq. (33a)] is obtained by introducing a new function F defined as follows:

$$F(c_D, c_T, G_D(\epsilon)) \equiv \hat{F}(c_D, c_T, 1/\epsilon). \quad (34)$$

This choice of form for F is motivated by the results of GAF.¹⁸ Using diagrammatic methods they obtained a resummation procedure by replacing $1/\epsilon$ by G_0 in the COP kernel analogous to F . This postulate implies that F depends on ϵ only through G_D and has further an implicit density dependence again through G_D . Other choices for

F are also possible.³³ In order to get an explicit expression for F , we expand it in density in two stages. First a naive expansion with respect to the explicit density dependence in F is made. This expansion is analogous to Eq. (33a), namely,

$$F(c_D, c_T, G_D) = \sum_{n,m=0}^\infty c_D^m c_T^n F^{(m,n)}(G_D). \quad (35)$$

Upon expansion of each $F^{(m,n)}$ in powers of $[G_D(\epsilon) - \epsilon^{-1}]$, assuming all $F^{(m,n)}$ are analytic functions of G_D , and making use of the naive expansion of $G_D(\epsilon)$, we obtain a systematic density expansion of $F^{(m,n)}$. The $O(c^2)$ results are given in Appendix B. Upon the substitution of Eqs. (34) and (35) into Eq. (32) we finally obtain

$$G_D(t) = \exp \left[\frac{1}{2\pi} \int_{-\infty}^\infty \frac{d\epsilon}{\epsilon^2} \exp(i\epsilon t) \times \sum_{n,m=0}^\infty c_D^m c_T^n F^{(m,n)}(G_D(i\epsilon)) \right], \quad (36a)$$

where

$$G_D(i\epsilon) = \int_0^\infty d\tau \exp(-i\epsilon\tau) G_D(\tau). \quad (36b)$$

Equations (36) are our most general SCE for $G_D(t)$. We recall that $F^{(n,m)}$ are known functions of G_D (see Appendix B). Equations (36) are exact, provided the summation in the rhs of Eq. (36a) is carried out to infinity. In practice, however, this expansion will be truncated and the SCE will be approximate. If we consider only two-body terms, and recalling Eqs. (28) and (29), we finally obtain

$$G_0(t) \equiv G_T(t)G_D(t), \quad (37a)$$

$$G_T(t) = \exp \left[-c_T \int_0^\infty d\vec{r} \{1 - \exp[-W(\vec{r})t]\} \right], \quad (37b)$$

and

$$G_D(t) = \exp \left[c_{D/2\pi} \int_{-\infty}^\infty \frac{\exp(i\epsilon t)}{\epsilon^2} \times \int d\vec{r} \frac{W(\vec{r})}{1 + 2W(\vec{r})G_D(i\epsilon)} \right], \quad (37c)$$

where $G_D(i\epsilon)$ is defined in Eq. (36b). Equations (37) are our final SCE within the two-body POP scheme. They will be solved in Sec. V for some model systems. Once we have this solution, it will enable us to solve for the mean-square displacement.

An approximate relation between the mean-square displacement $\langle r^2(t) \rangle$ and G_0 has already been found in the long-wavelength limit [see Eq. (24)]. It predicts the qualitatively reasonable result that when at long times $G_0(t) \rightarrow 0$ then $\langle r^2(t) \rangle \rightarrow \infty$. The mean-square displacement is also related to the generalized diffusion coefficient by Eq. (19). Using this, another relation between G_0 and the second moment can be established. This is done by making use of the low-density (cluster) expansion for D [Eq. (17)] and carrying out a partial resummation similar to that done in the development of the SCE [Eq. (37)].

The method is outlined in Appendix C and results in a hierarchy of resummed equations. The lowest-order (two-body) approximation is

$$D(k, c_D, G_D(\epsilon)) = -k^{-2} \int d\vec{r} [\exp(i\vec{k} \cdot \vec{r}) - 1] \times \frac{W(r)}{1 + 2W(r)G_D(\epsilon)}. \quad (38)$$

Making use of Eqs. (19) and (38) we then obtain

$$\langle r^2(\epsilon) \rangle = \epsilon^{-2} c_D r_0^2 \int dr r^{d+1} \frac{W(r)}{1 + 2W(r)G_D(\epsilon)}. \quad (39)$$

Explicit calculations for $\langle r^2(\epsilon) \rangle$ using Eq. (39) will be presented in Sec. V.

IV. THE COP SELF-CONSISTENT EQUATION

In this section we present the SCE obtained using the COP formulation [Eq. (2a) in the case of $G_0(t)$]. The derivation is analogous to the POP derivation, and the SCE [Eq. (45)] obtained is identical to that obtained by GAF using diagrammatic techniques. Here we present a brief outline of the procedure. In the next section the solutions of the two equations are compared. The COP derivation is based on the following REM for $G_0(t)$ and $G(k, t)$:

$$\frac{dG_0(t)}{dt} = \int_0^t d\tau \tilde{H}(t-\tau) G_0(\tau), \quad (40)$$

with the solution

$$G_0(\epsilon) = \frac{1}{\epsilon + \tilde{H}(\epsilon)} \quad (41)$$

and

$$\frac{dG(\vec{k}, t)}{dt} = -k^2 \int_0^t d\tau \Sigma(\vec{k}, t-\tau) G(\vec{k}, \tau), \quad (42)$$

with the solution

$$G(\vec{k}, \epsilon) = \frac{1}{\epsilon + k^2 \Sigma(\vec{k}, \epsilon)}. \quad (43)$$

Here ϵ is the Laplace transform variable conjugate to t and the COP kernels \tilde{H} and Σ have explicit expressions in terms of the original rate matrix W and appropriate projection operators.²⁹

To apply the density resummation technique of Sec. III we postulate the following forms:

$$G_0(c_D, c_T, \epsilon) = \frac{1}{\epsilon + \hat{H}(c_D, c_T, 1/\epsilon)} \equiv \frac{1}{\epsilon + H(c_D, c_T, G_0(\epsilon))}. \quad (44)$$

A density expansion may then be obtained for H , using the naive expansion of G_0 . Repeating the procedure used in Sec. III, we obtain the following SCE for G at the two-body level:¹⁸

$$[G_0(\epsilon)]^{-1} = \epsilon + \int d\vec{r} W(r) \left[\frac{c_D}{1 + 2W(r)G_0(\epsilon)} + \frac{c_T}{1 + W(r)G_0(\epsilon)} \right]. \quad (45)$$

We note that here [unlike in Eq. (37)] the donor and trap contributions enter identically except for a factor of 2. The density expansion used here also reproduces the three-body terms found by GAF and LAF and we have not repeated the derivation here.

An expression for the mean-square displacement in COP formalism is obtained by applying the same density expansion outlined in Appendix C to Eq. (43). The resulting expression is identical to the POP expression obtained in Eq. (39) except that now $G_D(\epsilon)$ is the solution of the COP SCE. Equation (39) is identical to that obtained by GAF.

V. SOLUTION OF THE SELF-CONSISTENT EQUATIONS

We are now in a position to solve the SCE [Eq. (37) or (45)] for specific model systems and analyze the behavior of $G_0(t)$ and $\langle r^2(t) \rangle$. We have considered the following models for $W(r)$:

(i) Power-law (multipolar) rate which commonly appears in energy-transfer problems:

$$W(r) = W_0 (r_0/r)^m, \quad m \geq 6. \quad (46)$$

(ii) Exponential (or exchange) transfer rate which appears, e.g., in electron-transfer problems:

$$W(r) = W_0 \exp(-r/r_0). \quad (47)$$

(iii) A step-function transfer rate:³⁴

$$W(r) = \begin{cases} W_0, & r < r_0 \\ 0, & r > r_0. \end{cases} \quad (48)$$

We note that model (iii), unlike models (i) and (ii), exhibits an upper cutoff (i.e., W vanishes for $r > r_0$). We shall later show that the presence of an upper cutoff is crucial for the existence of a percolation-type critical point in this model. In Eqs. (46)–(48), r_0 and W_0 are the characteristic range and magnitude of the transfer rate, respectively. Hereafter we shall use dimensionless units and set

$$W_0 = r_0 = 1, \quad (49)$$

i.e., r stands for r/r_0 and t for $W_0 t$. Moreover, c_D and c_T now also become dimensionless and are the number of donors and traps in a d -dimensional sphere of radius r_0 .

Let us consider first $G_T(t)$. Substituting the rates (i)–(iii) into Eq. (37b) we obtain²³ as $t \rightarrow \infty$

$$G_T(t) = \begin{cases} \exp[-c_T t^{d/m} \Gamma(1-d/m)], & \text{rate (i)} \\ \exp[-c_T (\ln t)^d], & \text{rate (ii)} \\ \exp(-c_T), & \text{rate (iii)}. \end{cases} \quad (50)$$

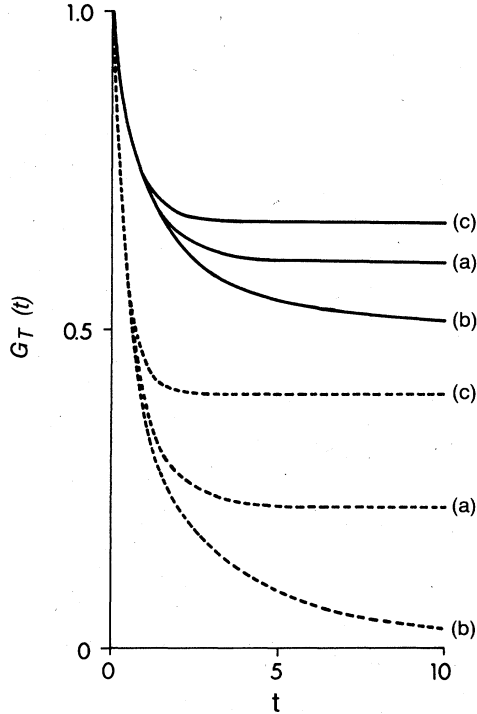


FIG. 1. Comparison of the POP and COP calculations of $G_T(t)$ for the step-function rate [Eq. (48)]. The dashed curves are for $c_T=1.5$, the solid curves for $c_T=0.5$. (a) POP exact result [Eq. (37b)]. (b) The solution of the COP SCE [Eq. (46)]. (c) COP "naive kernel," i.e., Eq. (44) with \hat{H} evaluated to first order in c . Note that the COP solution has a "critical point" at $c^*=1$ so that for $c=1.5$, G_T vanishes at long times whereas the exact solution is $\exp(-c_T)$.

Rate (ii) in Eq. (50) is the long-time asymptotic solution. The complete solution can be found in terms of Fermi-Dirac functions.³⁵ We see that $G_0(t)$ vanishes at long times for models (i) and (ii). The result of (iii) is straightforward since it is the probability for all traps to lie out-

$$A \exp(-Bt) = \exp \left[-dc \int_0^\infty dr r^{d-1} W \left\{ \frac{Bt}{B+2AW} - \frac{2AW}{(B+2AW)^2} \{ \exp[-(B+2AW)t] - 1 \} \right\} \right]. \quad (53)$$

If $B > 0$ we obtain, upon taking the long-time limit of Eq. (53),

$$B = dc \int_0^\infty dr r^{d-1} \frac{W}{1+2WA/B}, \quad (54a)$$

$$-\ln A = \frac{2dcA}{B^2} \int_0^\infty dr r^{d-1} \left[\frac{W}{1+2WA/B} \right]^2. \quad (54b)$$

For the COP SCE [Eq. (45)] we again postulate solutions of the form (51) and (52) and obtain the following SCE:³⁷

$$\frac{B}{A} = dc \int_0^\infty dr r^{d-1} \frac{W}{1+2WA/B}, \quad (55a)$$

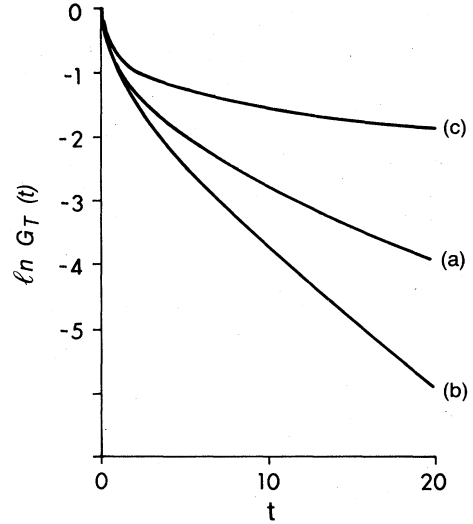


FIG. 2. Same as Fig. 1, but for the power-law rate [Eq. (46)] $m=6$, $c_T=0.5$.

side the range r_0 of the initial donor.

The COP [Eq. (45)] for traps only will not be analyzed here since a complete analysis for donors only is given in the next section and the traps-only case follows from that analysis by deleting the factor of 2. In Figs. 1 and 2 we compare the results of the two prescriptions for the calculation of G_T [Eqs. (37b) and (45)]. We shall now turn to the case of donors only ($c_T=0$, c_D finite). For the sake of brevity we shall hereafter denote c_D simply by c .

We begin by postulating the long-time solution³⁶

$$G_D(t) = A \exp(-Bt), \quad A, B > 0, \quad t \rightarrow \infty \quad (51)$$

or

$$G_D(\epsilon) = \frac{A}{\epsilon + B}. \quad (52)$$

The POP SCE [Eq. (37)] becomes

$$\frac{1}{A} - 1 = \frac{2dcA}{B^2} \int_0^\infty dr r^{d-1} \left[\frac{W}{1+2WA/B} \right]^2. \quad (55b)$$

Equations (54) and (55) are coupled equations for A and B , whose solution will give the asymptotic (long-time) behavior of $G_0(t)$ [Eq. (51)].

In order to explore the existence of solutions to Eq. (54) we define the function

$$I(A, B, R) \equiv d \int_0^R dr r^{d-1} \left[\frac{W}{1+2WA/B} \right], \quad (56)$$

and Eq. (54) becomes

$$B = I(A, B, \infty). \tag{57}$$

Equation (57) is graphically illustrated in Fig. 3. The important properties of $I(A, B, R)$ are that it is bounded for all $W(r)$ and R (assuming A is bounded) and that the slope $\partial I / \partial B$ at $B=0$ is infinite for rates without a cutoff, e.g., (i) and (ii) and finite for rates with cutoff, e.g., (iii). These properties ensure that a positive finite solution for B always exists for rates without a cutoff and thus these solutions are always "extended." For rates with cutoff, a positive solution B exists only if the slope at $B=0$ exceeds unity. Thus in this case it is possible to find both localized ($B=0$) and extended ($B>0$) solutions, depending on the value of c . A consistency check of this analysis is provided by noting that if we postulate $B=0$ in Eq. (53), the rhs remains time dependent with exponential terms as in Eq. (50) for models (i) and (ii), and the SCE is violated. This further confirms that localized solutions do not exist in these cases.

This analysis holds for the COP equations also, but for models (i) and (iii) it is possible to solve for $G_0(\epsilon)$ exactly and Eq. (55) is needed for model (ii) only.

For the power law (i) with $m=6$ we find, upon solving Eqs. (54),

$$B = \frac{\pi c^2}{8} e^{1/2}, \tag{58a}$$

$$A = e^{-1/2}. \tag{58b}$$

The corresponding COP equations (55) yield³⁸

$$B = \frac{\pi^2 c^2}{16}, \tag{59a}$$

$$A = \frac{1}{2}. \tag{59b}$$

For the exponential rate (ii) numerical solutions are required. The solutions for A and B are shown in Figs. 4 and 5. The important point to note is that B is always

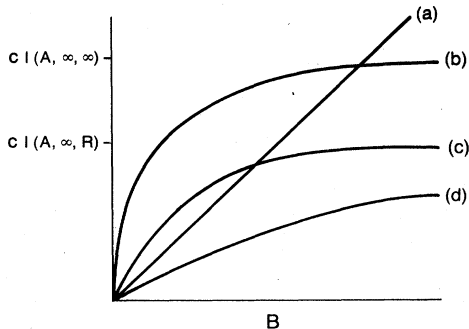


FIG. 3. Graphical solution of Eq. (57), in search of an extended solution. The straight line (a) is $y=B$. Curve (b) is $y=cI(A, B, \infty)$. For donors ($c=c_D$) its intersection with line (a) is the solution B for a transfer rate with no cutoff. Since dy/dB at $B=0$ is ∞ , there is always a solution for B for all values of c . Curve (c) is $y=cI(A, B, R)$ for $c > c^*$, and curve (d) the same function for $c < c^*$, both for a transfer rate with cutoff. We note that for (c) there is a solution for B , and no solution for (d). The figure is schematic and applies for general transfer rates.

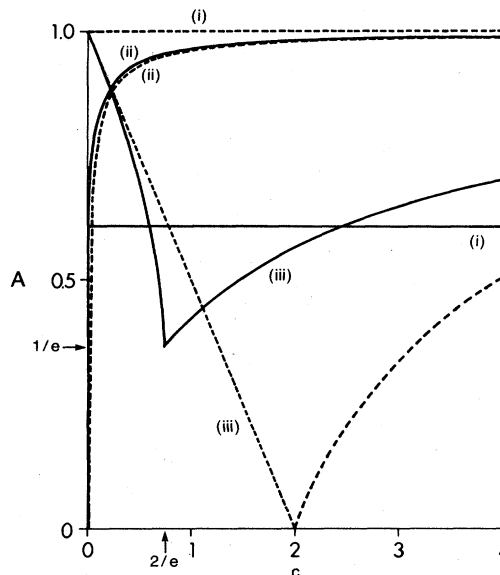


FIG. 4. Self-consistent solution for A as a function of donor concentration c . The solid curves represent the solution of Eq. (54) (POP) and the dashed curves show the solution of Eq. (55) (COP). The transfer rates are models (i)–(iii) [Eqs. (46)–(48)] as indicated in the figure. For model (i) we took $m=6$. Only model (iii) shows a critical point.

finite and that there is no critical behavior for cases (i) and (ii).

The long-time behavior of $\langle r^2(t) \rangle$ is found by substituting the asymptotic form [Eq. (51)] into Eq. (39), which is identical for the POP and COP. For $B > 0$, we obtain

$$\langle r^2(t) \rangle \sim tcd \int_0^\infty dr r^{d+1} \frac{W(r)}{1 + 2W(r)A/B}, \tag{60}$$

which shows that for the extended solutions, the behavior is diffusive. For the power law (i), Eq. (60) results in

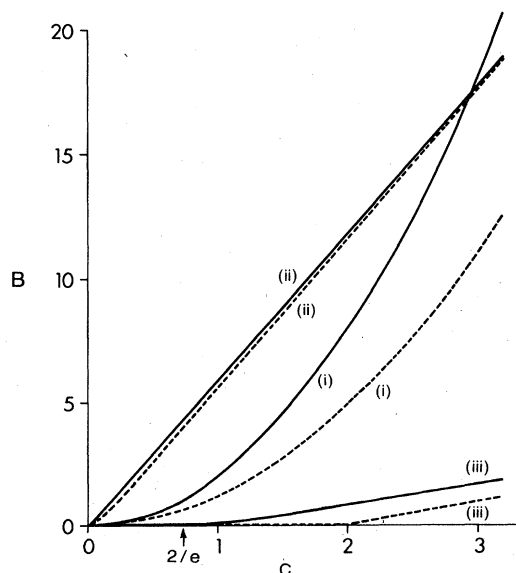


FIG. 5. Self-consistent solution of Eqs. (54) and (55) for B as a function of c . For details see the caption to Fig. 4.

$$\langle r^2(t) \rangle = \frac{1}{6} \left(\frac{2A}{B} \right)^{(d+2-m)/m} \beta \left[\frac{d+2}{m}, \frac{m-d-2}{m} \right] t, \tag{61a}$$

where the β function is given by

$$\beta \left[\frac{d+2}{m}, \frac{m-d-2}{m} \right] = \int_0^\infty dy y^{(d+2-m)/m} (y+1)^{-1}. \tag{61b}$$

For $d=3$ and $m=6$ we obtain

$$\langle r^2(t) \rangle = t \frac{1}{6} \left(\frac{2A}{B} \right)^{-1/6} \beta \left(\frac{5}{6}, \frac{1}{6} \right). \tag{61c}$$

Equation (61c) together with (59) is identical to that of GAF.¹⁸ The only difference between the COP and the POP resummation will be in the value of A/B [Eqs. (58) and (59)] which differ by $\sim 10\%$. If $B=0$, we obtain the localized solution,

$$\langle r^2(t) \rangle \sim \frac{d}{d+2} \frac{c}{2A}, \quad t \rightarrow \infty \tag{61d}$$

assuming that $W(r)$ has an upper cutoff.

To obtain the entire time evolution of $G_0(t)$, we have solved the SCE's (37c) and (45) iteratively. The iteration was done by making a zeroth order approximation $G_0(\epsilon) = 1/\epsilon$ on the rhs of Eqs. (37c) or (45) and then repeatedly iterating until convergence was obtained. The converged solution was substituted into Eq. (39) giving

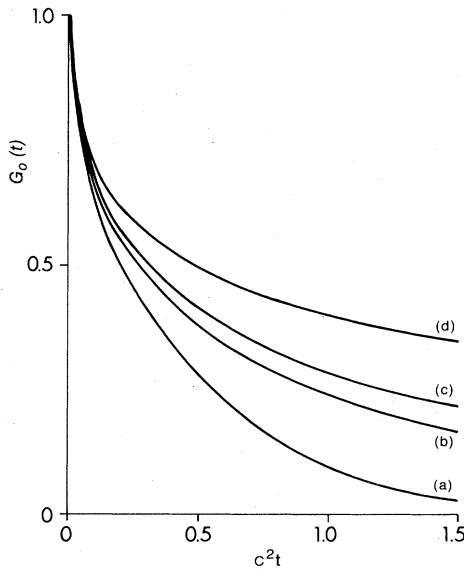


FIG. 6. Solutions of the SCE's (37) and (45) for the power-law rate [Eq. (46)]; $m=6$. Note that the dependence on c is simply via scaling of the time. The various curves are (a) POP SCE [Eq. (37)]; (b) COP SCE [Eq. (45)]; (c) POP "naive kernel," i.e., Eq. (32) with \hat{F} [Eq. (33a)] evaluated to first order in c (Refs. 20 and 39), i.e., $G_0(t) = \exp[-(c/2)(2t)^{d/m} \Gamma(1-d/m)]$ with $d=3$, $m=6$; (d) COP "naive kernel," i.e., Eq. (44) with \hat{H} evaluated to first order in c .

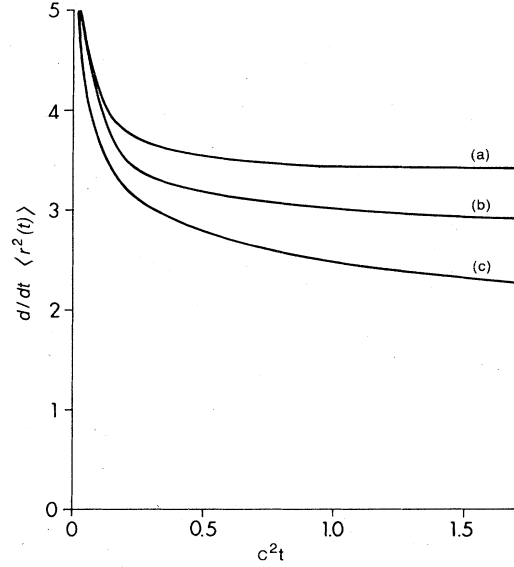


FIG. 7. Rate of change of the second moment [Eq. (39)] for the power-law rate [Eq. (46) with $m=6$]. $G_D(\epsilon)$ in Eq. (39) was calculated as follows. (a) Self-consistent solution of Eq. (37) (POP); (b) Self-consistent solution of Eq. (45) (COP); (c) First order in c [setting $G_D = 1/\epsilon$ in Eq. (39)]. This calculation is identical for the POP and the COP.

$\langle r^2(t) \rangle$ at all t . The results for model (i) are shown in Figs. 6 and 7, and for model (ii) in Figs. 8 and 9. They agree at long times with the above asymptotic analysis. To demonstrate the effect of the resummation procedure we also show calculations obtained using the "naive" kernels only, i.e., Eq. (33a) with \hat{F} to linear order in c and Eq. (44) with \hat{H} first order in c .³⁹

We now turn to the analysis of model (iii), the step-function rate. We first discuss the POP results and then

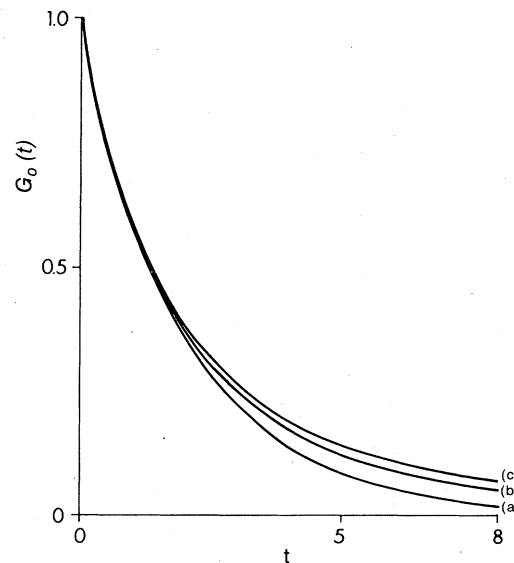


FIG. 8. Same as Fig. 6 but for the exponential rate [Eq. (47)]. $c=0.1$. Calculations (a), (b), and (c) correspond to curves (a), (b), and (c), respectively, in Fig. 6.

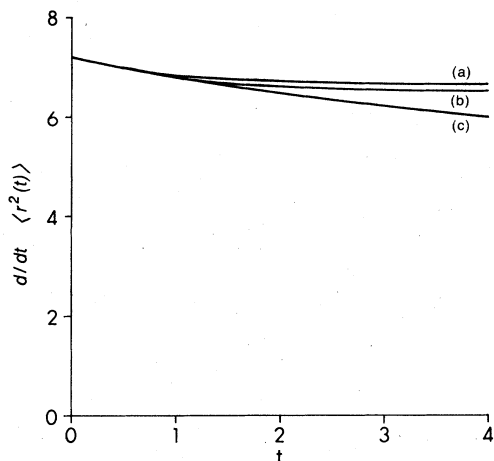


FIG. 9. Same as Fig. 7 but for the exponential rate [Eq. (47)].

the COP results. Starting with the long-time analysis, we postulate a localized solution ($B = 0$) in Eq. (53), resulting in

$$A = \exp(-c/2A) \tag{62}$$

which can be solved iteratively, giving

$$A = \exp\left[-\frac{c}{2}x\right], \tag{63a}$$

$$x = \exp\left\{\frac{c}{2}\exp\left[\frac{c}{2}\exp\left[\frac{c}{2}\dots\right]\right]\right\}. \tag{63b}$$

A graphical examination of the iteration procedure is shown in Fig. 10. If $c < 2/e$, the curve $y = \exp(-c/2A)$ intersects $y = A$ at $A = 0$, P , and Q where $P, Q < 1$. Thus for all $A_0 > P$ the iteration limit point is at $A = Q$, while for all $A_0 < P$ the limit point is at $A = 0$. For $c > 2/e$ the

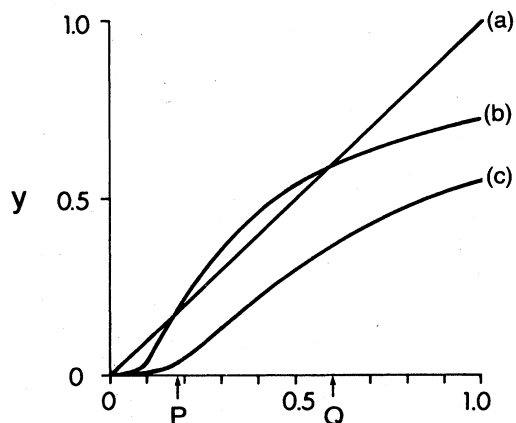


FIG. 10. Graphical solution of Eq. (62) in search of a localized solution for any transfer rate $W(r)$ with a cutoff [e.g., model (iii)]. The straight line (a) is $y = A$. Curve (b) is $y = \exp(-c/2A)$ for $c < 2/e$ ($c = 0.6$). Its intersection point Q with line (a) is the stable solution whereas point P is an unstable solution. Curve (c) shows y for $c > 2/e$ ($c = 1.2$). It intersects the line (a) only at the origin, and the only solution is $A = 0$.

only limit point occurs at $A = 0$. For $c = 2/e$ the limit points are $A = 1/e$ and 0. Thus the iteration method gives the following results for all transfer rates with cutoff in all dimensions: For $c < 2/e$, $G_D(\infty)$ is finite and nonzero. For $c > 2/e$, $G_D(\infty)$ is zero.

For $B > 0$, Eq. (53) results in

$$B = c - 2A \tag{64a}$$

and

$$A = \exp(-2A/c), \tag{64b}$$

whose iterative solution is

$$A = \exp\left\{-\frac{2}{c}\exp\left[-\frac{2}{c}\exp\left[-\frac{2}{c}\dots\right]\right]\right\}. \tag{65}$$

Equations (63)–(65) clearly show the existence of a percolation-type critical point at $c^* \equiv 2/e$ for which $A^* = 1/e$ and $B^* = 0$. Below the critical point, $c < c^*$, the appropriate solution is given by Eq. (63) since Eq. (64) gives an unphysical solution whereby B is negative. In this region, A [as given by Eq. (64b)], varies from $A = 1$ for $c = 0$ to $A = 1/e$ for $c = c^*$, and the long-time solution is localized. For $c > c^*$ the solution is extended. The results for A and B for the step-function rate are shown in Figs. 4 and 5. The entire time dependence of $G_0(t)$ and $\langle r^2(t) \rangle$ was again found by repeated iteration of the SCE (37), and the results are shown in Figs. 11–14 and agree at long times with the results of this asymptotic analysis.

A good approximation for the converged solution of $G_0(t)$ may be obtained by substituting the asymptotic form [Eq. (51)] on the rhs of Eq. (37), resulting in

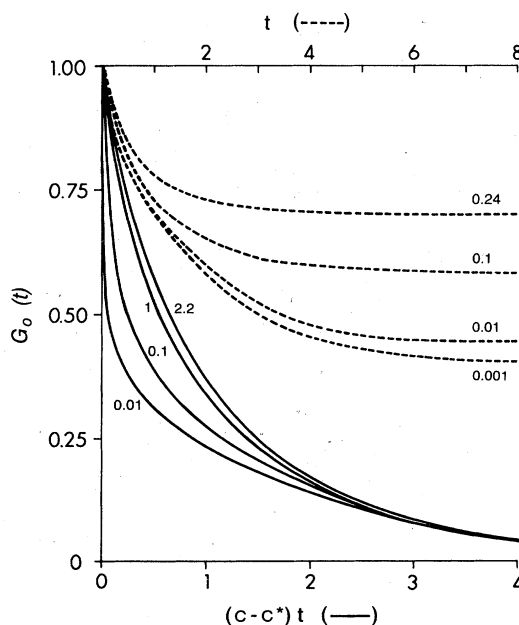


FIG. 11. Converged solution of the POP SCE [Eq. (37)] for the step-function rate [Eq. (48)] $c^* = 2/e$. The dashed curves correspond to $c < c^*$ and the time axis is shown on the top. The solid curves are for $c > c^*$. The time axis as shown on the bottom is scaled by $c - c^*$. The values of $|c - c^*|$ are shown.

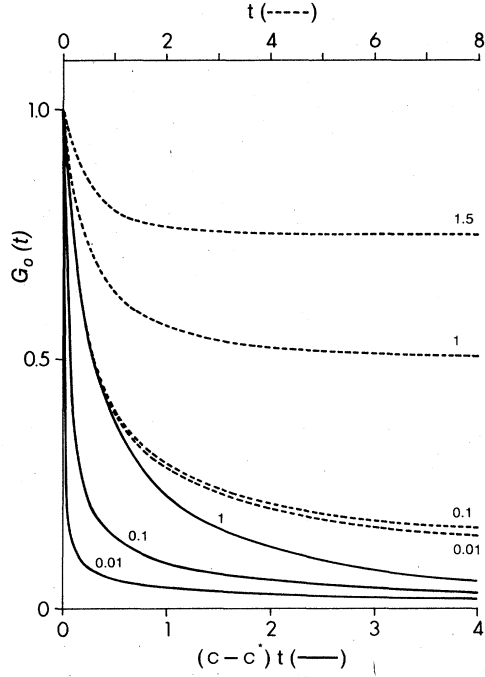


FIG. 12. Same as Fig. 11, but using the COP SCE [Eq. (45)]. $c^* = 2$. The dashed curves represent $c < c^*$ with the upper time axis. The solid curves are for $c > c^*$ and the time axis is shown at the bottom. The values of $|c - c^*|$ are shown.

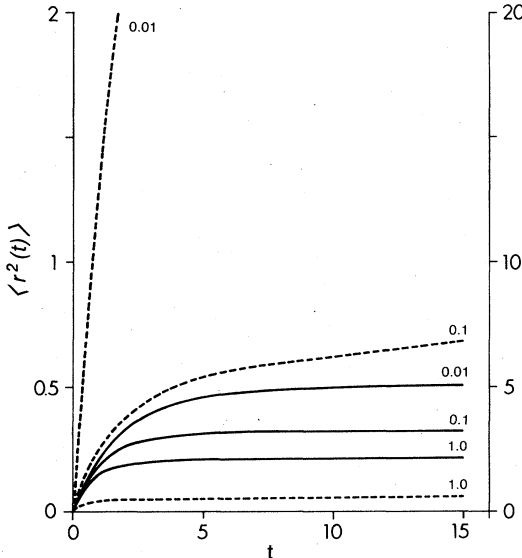


FIG. 13. The second moment $\langle r^2(t) \rangle$ [Eq. (39)] for the step-function rate (48) in the localized region $c < c^*$. The solid curves are the POP $G_0(\epsilon)$ [i.e., solution of Eq. (37c)] and correspond to the vertical left axis. The dashed curves use the COP solution for $G_0(\epsilon)$ [i.e., solution of Eq. (45)] and correspond to the right vertical axis. The values of $c^* - c$ are shown in the figure.

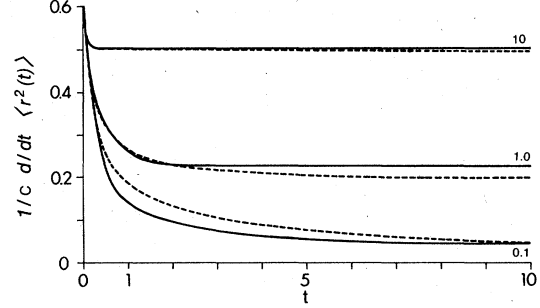


FIG. 14. The time derivative of the second moment for $c > c^*$. Calculations are similar to Fig. 13. Values of $c - c^*$ are shown. Solid curves, POP; dashed curves, COP.

$$G_0(t) = \exp \left[-\frac{c}{2A} [1 - \exp(-2At)] \right], \quad c < c^* \quad (66a)$$

and

$$G_0(t) = \exp \left[-\frac{(c-2A)t}{c} - \frac{2A}{c} [1 - \exp(-2ct)] \right], \quad c > c^*. \quad (66b)$$

We now turn to the COP analysis for the step-function rates. The SCE (45) now has the solution

$$G_0(\epsilon) = \frac{1}{4\epsilon} \{ 2 - c - \epsilon + [(2 - \epsilon - c)^2 + 8\epsilon]^{1/2} \}, \quad (67)$$

which has a critical point $c^* = 2$. Using this exact solution or Eq. (55) we obtain the following long-time results: $A^* = 0$, $B^* = 0$ and above the critical point $c > c^*$

$$A = 1 - \frac{2}{c}, \quad (68a)$$

$$B = \frac{(c-2)^2}{c}, \quad (68b)$$

whereas below the critical point $c < c^*$

$$B = 0, \quad (69a)$$

$$A = 1 - \frac{c}{2}. \quad (69b)$$

At the critical point $c = c^*$, $G_0(t)$ decays algebraically at long time as

$$G_0(t) \sim (\pi\eta t)^{-1/2}. \quad (70)$$

The entire time dependence of $G_0(t)$ is shown in Fig. 12 and that of $\langle r^2(t) \rangle$ in Figs. 13 and 14.

VI. THE THREE-BODY SCE

We have further investigated the resulting SCE obtained by including the three-body terms. For the sake of simplicity we shall restrict ourselves to the COP formalism and to models (i) and (ii). The expressions for the three-body COP terms were given by GAF. The resulting expression for the naive expansion is

$$\epsilon G_0 = 1 - c(\epsilon+2)^{-1} + c^2(\epsilon+x)(\epsilon+1)^{-1} \times (\epsilon+2)^{-1}(\epsilon+3)^{-1}, \quad (71)$$

where x is a dimensionally dependent volume fraction given by (1D, 2D, and 3D represent one, two, and three dimensions, respectively)

$$x = \begin{cases} \frac{5}{4} & \text{for 1D,} \\ 1 + \sqrt{27/4}\pi & \text{for 2D,} \\ \frac{49}{32} & \text{for 3D.} \end{cases} \quad (72)$$

Transforming (71) to the time domain and considering the $t \rightarrow \infty$ limit, we obtain

$$G_0(t) = 1 - \frac{1}{2}c + \frac{1}{6}xc^2 + \dots \quad (73)$$

Note that this result can also be obtained by simple probabilistic arguments, since the probability $p(n)$ of finding n particles in a $V(d)$ about the origin is a Poisson distribution, and including contributions up to three bodies the result is

$$G_0(t) \sim \sum_{n=0}^2 \frac{1}{n!} c^n \exp(-c) \quad (74)$$

Upon expanding Eq. (74) in density, we obtain Eq. (73) with $x = 1$. The three-body COP SCE is

$$G_0^{-1} = \epsilon + c(1 + 2G_0)^{-1} + c^2 \left[\frac{G_0 + xG_0^2}{(1 + G_0)(1 + 2G_0)(1 + 3G_0)} + \frac{G_0}{(1 + 2G_0)^3} \right] \quad (75)$$

Equation (75) is a sixth-order equation for $G_0(\epsilon)$. For the long-time limit, we again postulate the exponential form (52) and the resulting equation for A/B is a fifth-order equation which we write as

$$\sum_{n=0}^5 a_n \left(\frac{A}{B} \right)^n = 0 \quad (76)$$

The coefficients a_n depend on c and x only. Close to the critical point (assuming it exists), B must tend to zero. Thus keeping only the highest powers in A/B , we find

$$\frac{A}{B} \simeq -\frac{a_4}{a_5} \quad (77)$$

where

$$a_5 = -24 + 12c + 4xc^2, \quad (78a)$$

$$a_4 = -68 + 28c + (7 + 4x)c^2, \quad (78b)$$

and consequently the critical point c^* should occur where $a_5 \simeq 0$ if $B \rightarrow 0$. Using Eq. (55b), resulting from $O(\epsilon)$ terms in the expansion of (76) we obtain that

$$A \simeq \frac{a_5}{24}, \quad (79a)$$

$$B \simeq -\frac{a_5^2}{24a_4}, \quad (79b)$$

where $a_4 < 0$ if $a_5 \simeq 0$.

These estimates were confirmed by making a computer search for the roots of Eq. (76). The numerical results show that only for $c > c^*$ does one real, positive root of

(76) exist.

The three-body results thus confirm that the existence of localized and extended regions is not only a two-body phenomenon. However, the inclusion of the three-body terms modifies the position of the critical point c^* , which is now found to be dimensionally dependent, and is

$$c^* = \begin{cases} 1.30 & \text{for 1D,} \\ 1.26 & \text{for 2D,} \\ 1.23 & \text{for 3D.} \end{cases} \quad (80)$$

In Fig. 15 we show the solutions of A and B and compare them with the two-body SCE. By contrast, for the power-law rate ($m = 6$), for which it is easy to obtain an exact expression for the $G_0(t)$, the solution is still extended. The expression is

$$G_0(t) = (1 + 2\alpha t) \operatorname{erfc}(\sqrt{\alpha t}) \exp(\beta t) - 2 \left(\frac{\alpha t}{\pi} \right)^{1/2} \exp(\beta t - \alpha t), \quad (81)$$

where

$$\alpha = \frac{\pi^2}{16} c^2, \quad (81a)$$

$$\beta = 0.18c^2. \quad (81b)$$

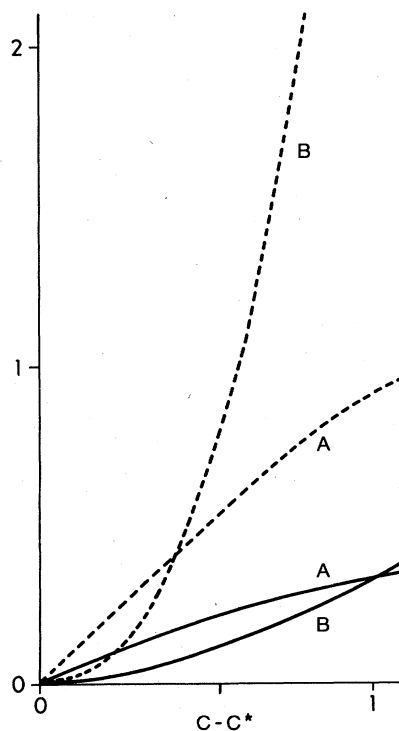


FIG. 15. A comparison of the long-time solutions of the two-body equations (55) and the three-body equations (76) for the step-function rate (48). The solid curves are the solutions of the two-body equation ($c^* = 2.0$), whereas the dashed curves correspond to the three-body equation ($c^* = 1.23$ in 3D).

β contains the effects of the three-body terms, whereas α is due to two-body terms only. erfc denotes the complementary error function, and by examining its asymptotic expansion, it follows that $G_0(t)$ still decays exponentially at long times.

For the sake of comparison, the three-body POP equation is

$$G_D(t) = \exp(\beta c^2 t) \exp \left[\frac{1}{2\pi} \int_{-\infty}^{\infty} d\epsilon \frac{\exp(i\epsilon t)}{\epsilon^2} \times \frac{c}{2[2G_D(i\epsilon)]^{1/2}} \right] \quad (82)$$

with $\beta=0.148$. The addition of β in Eq. (82) or (81) is the only effect of the three-body terms.

VII. DISCUSSION

In this paper we studied the transport properties of disordered systems described by a master equation with transition rates which are random due to the random distribution of distances between donor particles. In particular we focused on $G_0(t)$, the probability of the excitation to return to its original site, and $\langle r^2(t) \rangle$ the second moment of the distribution of excitations. Our purpose was to obtain a good approximation for the long-time (low-frequency) behavior of these quantities. The method we developed is based on a systematic density expansion for $G_0(t)$ which is truncated at some finite order and then resummed to obtain a self-consistent approximation for $G_0(t)$ which is infinite order in density. Two resummation procedures were used. The first [Eq. (36)] is based on the time-convolutionless formalism POP and the second [Eq. (44)] is based on the conventional memory-type COP formalism and is identical with the GAF equation. To lowest order in density our SCE become Eqs. (37) and (45), respectively. Our derivation of the COP equation is somewhat simpler than the original derivation of GAF, since only the density expansion of $G_0(t)$ and not of the entire Green's function $G(k, t)$ is needed as an input to the equation. The POP equation has some clear advantages over the COP for the present problem. First, for the case of traps only ($c_D=0$, the Forster problem), the POP kernel \tilde{F} is exactly first order in density and our equation yields the exact result. The COP equation is approximate even in this simple case. Also the GAF equation treats traps and donors (c_T and c_D) in a very similar way [see Eq. (45)] whereas the POP equation factors out the trap only solution [see Eqs. (37)]. An extreme consequence of

this is shown in Fig. 1 where the POP curves are exact and $G_T(t)$ always vanishes at long times whereas the COP equation predicts an unphysical "critical point" which for $c < c^*$, $G_T(t)$ remains finite!

Once $G_0(t)$ is found we can calculate the second moment $\langle r^2(t) \rangle$ [and the diffusion coefficient $D(\omega)$] via Eq. (39). We have analyzed the solution of our SCE for three types of transfer rates $W(r)$: (i) $1/r^m$, (ii) $\exp(-r)$, and (iii) a step function [see Eqs. (46)–(48)]. For cases (i) and (ii) whereby $W(r)$ does not have an upper cutoff in r , we find that $G_0(t)$ always vanishes at long time ("extended" solution). The long-time behavior is exponential $\sim A \exp(-Bt)$ and A and B as a function of c are shown in Figs. 4 and 5. For the step-function rate (iii) which is a continuum percolation model, we find a critical point c^* whereby $c > c^*$, $G_0(t) \sim A \exp(-Bt)$, $t \rightarrow \infty$ with finite B whereas for $c < c^*$, $G_0(t) \sim A$ ("localized" solution), A and B are again shown in Figs. 4 and 5. No qualitative differences exist between the COP and POP resummations in this case although they are quantitatively different (c^* as well as A and B are different).

The present resummation schemes (POP or COP) yield the correct result for the long-time behavior of the second moment $\langle r^2(t) \rangle$, as well as the low-frequency diffusion constant. The results are similar to those of the CPA (Refs. 15, 16, 40, and 41) the continuous-time random walk,^{6,22,42,43} and scaling arguments.^{44,45} The exponential behavior of $G_0(t)$ in the extended region differs, however, from the $t^{-d/2}$ obtained by these other methods. The reason is that the only input in the present resummation is the dynamics of small clusters, whereas the other resummation schemes make use of the exact Green's function of the ordered systems. Consequently, the other schemes contain the correct dimensionality dependence of $G_0(t)$ as well. This is clearly an advantage of the other resummation methods. Using the present resummation, the same degree of accuracy for $G_0(t)$ will be obtained only by going to much higher orders. We have further analyzed the next order (three-body second order in density) [Eq. (75)]. We found that the critical point predicted by the two-body approximation is stable to the addition of the three-body terms. The results did not change appreciably especially near the critical point.

ACKNOWLEDGMENT

The support of the National Science Foundation and the Petroleum Research Fund administered by the American Chemical Society is gratefully acknowledged. S.M. is a recipient of the Alfred P. Sloan fellowship and the Camille and Henry Dreyfus teacher scholarship.

APPENDIX A: THREE-BODY COEFFICIENTS OF $S^{(m,n)}$

In this appendix we give the expressions for the three-body coefficients $S^{(m,n)}$ of the naive expansion (25). The method of derivation is given by HZ and here we give only the final results [for brevity we write $w_{ij} \equiv w(r_{ij})$],

$$S^{(2,0)}(\epsilon) = -\frac{1}{\epsilon} \int d\vec{r}_{12} d\vec{r}_{13} \left[\frac{\frac{1}{\epsilon} w_{12} + (w_{12} w_{13} + w_{12} w_{23} + w_{13} w_{23}) \frac{1}{\epsilon^2}}{1 + \frac{2}{\epsilon} (w_{12} + w_{13} + w_{23}) + \frac{3}{\epsilon^2} (w_{12} w_{13} + w_{12} w_{23} + w_{13} w_{23})} - \frac{\frac{1}{\epsilon} w_{12}}{1 + \frac{2}{\epsilon} w_{12}} \right], \quad (A1)$$

$$S^{(1,1)}(\epsilon) = -\frac{1}{\epsilon} \int d\vec{r}_{12} d\vec{r}_{13} \left[\frac{(\epsilon + w_{12} + w_{32})\epsilon}{(\epsilon + w_{12} + w_{32})(\epsilon + w_{21} + w_{31}) - w_{21}^2} - \frac{\frac{1}{\epsilon} w_{31}}{1 + \frac{1}{\epsilon} w_{31}} \right], \quad (\text{A2})$$

$$S^{(0,2)}(\epsilon) = \frac{1}{\epsilon} \int d\vec{r}_{12} d\vec{r}_{13} \frac{w_{31} w_{21}}{(\epsilon + w_{21})(\epsilon + w_{21} + w_{31})}. \quad (\text{A3})$$

APPENDIX B: THREE-BODY TERMS $F^{(m,n)}$

In this appendix we give expressions for the three-body terms of the resummed kernel $F^{(m,n)}$ [see Eq. (35)]. These terms are obtained by the method described in the text.

The relations between the naive expansion kernels $S^{(m,n)}$, Eq. (25) and the "unsummed" kernels $\hat{F}^{(m,n)}$ of Eq. (33a) are found by expanding Eq. (32) and comparing powers of c_T and c_D . The relations for $m+n < 2$ are

$$\hat{F}^{(0,1)} = 0, \quad (\text{B1})$$

$$\hat{F}^{(1,0)} = -\epsilon^2 S^{(1,0)}(\epsilon), \quad (\text{B2})$$

$$\hat{F}^{(2,0)} = -\epsilon^2 S^{(2,0)}(\epsilon) + \frac{\epsilon^2}{2} \int_0^\infty dt \exp(-\epsilon t) \times [S^{(1,0)}(t)]^2, \quad (\text{B3})$$

$$\hat{F}^{(1,1)} = -\epsilon^2 S^{(1,1)}(\epsilon) + \epsilon^2 \int_0^\infty dt \exp(-\epsilon t) S^{(0,1)}(t) S^{(1,0)}(t), \quad (\text{B4})$$

$$\hat{F}^{(0,2)} = 0. \quad (\text{B5})$$

The relations between the resummed kernels $F^{(m,n)}$ and

the kernels $\hat{F}^{(m,n)}$ are obtained by inserting the naive expansion for $G_0(\epsilon)$ into each term $F^{(m,n)}$ of Eq. (35), making a Taylor-series expansion of each term about $c=0$ and using Eq. (34) to compare powers of c_T, c_D with the expansion of \hat{F} . The relations between $F^{(m,n)}$ and $\hat{F}^{(m,n)}$ for $m+n \leq 2$ are

$$\hat{F}^{(0,1)}|_{\rho=0} = 0, \quad (\text{B6})$$

$$\hat{F}^{(1,0)}|_{\rho=0} = \hat{F}^{(1,0)} = \int d\vec{r} \frac{w_{12}(r)}{1 + 2w_{12}(r)(1/\epsilon)}, \quad (\text{B7})$$

$$\hat{F}^{(2,0)} = \left[F^{(2,0)}(G_0) + S^{(1,0)}(\epsilon) \frac{\partial F^{(1,0)}}{\partial G_0} \right]_{c=0}, \quad (\text{B8})$$

$$\hat{F}^{(1,1)} = \left[F^{(1,1)}(G_0) + S^{(0,1)}(\epsilon) \frac{\partial F^{(1,0)}}{\partial G_0} + S^{(1,0)}(\epsilon) \frac{\partial F^{(0,1)}}{\partial G_0} \right]_{c=0}, \quad (\text{B9})$$

$$\hat{F}^{(0,2)} = \left[F^{(0,2)}(G_0) + S^{(0,1)}(\epsilon) \frac{\partial F^{(0,1)}}{\partial G_0} \right]_{c=0}. \quad (\text{B10})$$

Substituting the previous results (B1)–(B5) into the above equations and relaxing the condition $c=0$, by setting $G_0 = 1/\epsilon$ (following GAF), we obtain the results

$$F^{(0,2)}(G_0) = 0, \quad (\text{B11})$$

$$F^{(2,0)} = -G_0^{-2} S^{(2,0)}(G_0^{-1}) - \frac{1}{8} G_0^{-1} \int d\vec{r}_{12} d\vec{r}_{13} \left[1 - \frac{2}{1 + 2w_{12}G_0} + \frac{1}{1 + 2(w_{12} + w_{13})G_0} \right] - 2G_0^{-2} \int d\vec{r}_{12} d\vec{r}_{13} \frac{w_{13}w_{12}^2}{(1 + 2w_{13}G_0)(1 + 2w_{12}G_0)^2}. \quad (\text{B12})$$

The second term on the rhs of (B12) is due to the product of two-body terms in (B3) and the third term due to the derivative term in (B8). Similarly, the expression for $F^{(1,1)}$ is

$$F^{(1,1)}(G_0) = -G_0^{-2} S^{(1,1)}(G_0^{-1}) - G_0^{-1} \int d\vec{r}_{12} d\vec{r}_{13} \frac{2G_0^{-1} w_{12} w_{13} + w_{12} w_{13} (2w_{12} + w_{13})}{(G_0^{-1} + w_{12})(G_0^{-1} + 2w_{13})(G_0^{-1} + w_{12} + 2w_{13})} - G_0^{-1} \int d\vec{r}_{12} d\vec{r}_{13} \frac{G_0 w_{21}}{1 + G_0 w_{21}} \frac{2G_0 w_{13} (1 + G_0 w_{13})}{(1 + 2G_0 w_{13})^2}. \quad (\text{B13})$$

APPENDIX C: A RESUMMED DENSITY EXPANSION OF $D(\vec{k}, t)$

The only input required to obtain a density expansion for the diffusion coefficient D is the naive expansion for

$G(\vec{k}, t)$, given by¹⁴

$$G(\vec{k}, t) = \sum_{m,n=0}^{\infty} c_D^n c_T^m B^{(n,m)}(\vec{k}, t), \quad (\text{C1})$$

where $B^{(0,0)} = 1$ and the coefficient $B^{(n,m)}$ is obtained by

calculating the rhs of (9) for a system consisting of $N + M + 1$ particles. $D(\vec{k}, t)$ is related to $G(\vec{k}, t)$ by Eq. (15). We assume the Laplace-transformed quantity $\hat{D}(\vec{k}, \epsilon)$ has an expansion similar to that of \hat{F} in (33), namely,

$$\hat{D}(\vec{k}, 1/\epsilon) = \sum_{m,n=0}^{\infty} c_D^n c_T^m \hat{D}^{(n,m)}(\vec{k}, 1/\epsilon) \quad (C2)$$

where $\hat{D}^{(0,0)} = 0$. Again we form a second function $\tilde{D}(\vec{k}, \rho, G_0(\epsilon))$, related to \hat{D} by

$$\tilde{D}(\vec{k}, c, G_0(\epsilon)) = \hat{D}(\vec{k}, c, 1/\epsilon), \quad (C3)$$

where \tilde{D} has the expansion

$$\tilde{D}(\vec{k}, c, G_0(\epsilon)) = \sum_{n,m=0}^{\infty} c_D^n c_T^m \tilde{D}^{(n,m)}(\vec{k}, G_0), \quad (C4)$$

and $\tilde{D}^{(0,0)} = 0$. The other coefficients $\tilde{D}^{(n,m)}$ are determined by expanding each in a Taylor series about $c = 0$ and then comparing the resulting density expansion to the naive expansion of $G(\vec{k}, t)$ (Ref. 14) through the relation (15). The expression for $\tilde{D}^{(1,0)}$, which is the only coefficient we require, is given in (57).

This procedure can be used identically for the COP form¹⁶

$$G(\vec{k}, \epsilon) = [\epsilon + k^2 \Sigma(k, 1/\epsilon)]^{-1} \\ = [\epsilon + k^2 \hat{\Sigma}(k, G_0(\epsilon))]^{-1}. \quad (C5)$$

The $O(c_D)$ coefficient $\hat{\Sigma}^{(1,0)}$ is identical to $\tilde{D}^{(1,0)}$. However, the higher terms will differ from $\tilde{D}^{(m,n)}$.

¹T. Forster, *Ann. Phys.* **2**, 55 (1948).

²D. L. Dexter, *J. Chem. Phys.* **21**, 836 (1953).

³S. Kirkpatrick, *Rev. Mod. Phys.* **45**, 574 (1973).

⁴B. Stauffer, *Phys. Rep.* **54**, 1 (1979).

⁵V. P. Sakun, *Fiz. Tverd. Tela (Leningrad)* **14**, 2199 (1972) [*Sov. Phys.—Solid State* **14**, 1906 (1973)].

⁶H. Scher and M. Lax, *Phys. Rev. B* **7**, 4491 (1973); **7**, 4502 (1973).

⁷R. Kopelman, E. M. Momborg, and F. W. Ochs, *Chem. Phys.* **19**, 413 (1977); **21**, 373 (1977).

⁸J. M. Ziman, *Models of Disorder* (Cambridge University Press, Cambridge, 1979).

⁹S. Alexander, J. Bernasconi, W. R. Schneider, and R. Orbach, *Rev. Mod. Phys.* **53**, 175 (1981); in *Physics in One Dimension*, Vol. 23 of *Springer Series in Solid State Science*, edited by J. Bernasconi and T. Schneider (Springer, Berlin, 1981), p. 277.

¹⁰See *Electrical Transport and Optical Properties of Inhomogeneous Media*, edited by J. C. Garland and D. B. Tanner (AIP, New York, 1978).

¹¹J. P. Straley, *Phys. Rev. B* **15**, 5733 (1977).

¹²I. Webman, J. Jortner, and M. H. Cohen, *Phys. Rev. B* **11**, 2885 (1975); **14**, 4737 (1976).

¹³M. H. Cohen, J. Jortner, and I. Webman, in *Electrical Transport and Optical Properties of Inhomogeneous Media*, Ref. 10, p. 63.

¹⁴S. W. Haan and R. Zwanzig, *J. Chem. Phys.* **68**, 1879 (1979); *J. Phys. A* **10**, 1547 (1977).

¹⁵T. Odagaki and M. Lax, *Phys. Rev. Lett.* **45**, 847 (1980); *Phys. Rev. B* **25**, 2307 (1982); **26**, 6480 (1980).

¹⁶I. Webman, *Phys. Rev. Lett.* **47**, 1496 (1981).

¹⁷B. Movaghar, M. Grunewald, B. Pohlmann, D. Wurtz, and W. Schirmacher, *J. Stat. Phys.* **39**, 315 (1983).

¹⁸R. C. Gouchanour, H. C. Andersen, and M. D. Fayer, *J. Chem. Phys.* **70**, 4254 (1979).

¹⁹R. F. Loring, H. C. Andersen, and M. D. Fayer, *J. Chem. Phys.* **76**, 2015 (1982); *Phys. Rev. Lett.* **50**, 1324 (1983).

²⁰K. Godzik and J. Jortner, *J. Chem. Phys.* **72**, 4471 (1980); *Chem. Phys. Lett.* **63**, 428 (1979).

²¹D. L. Huber, *Phys. Rev. B* **20**, 2307 (1979); D. L. Huber, D. S. Hamilton, and B. Barnett, *ibid.* **16**, 4642 (1977).

²²J. Klafter and R. Silbey, *J. Chem. Phys.* **72**, 849 (1980); **72**,

843 (1980).

²³A. Blumen, J. Klafter, and R. Silbey, *J. Chem. Phys.* **72**, 5320 (1980).

²⁴A. Blumen and R. Silbey, *J. Chem. Phys.* **70**, 3707 (1979); A. Blumen, *J. Chem. Phys.* **72**, 2632 (1980).

²⁵R. B. Stinchcombe and B. P. Watson, *J. Phys. C* **9**, 3221 (1976).

²⁶J. Machta, *Phys. Rev. B* **24**, 5260 (1981).

²⁷S. Mukamel, (a) *Adv. Chem. Phys.* **47**, 509 (1981); (b) *Phys. Rev. A* **26**, 617 (1982); (c) *J. Chem. Phys.* **75**, 159 (1981); (d) *Phys. Rev. B* **25**, 830 (1982).

²⁸S. Abe and S. Mukamel, *J. Chem. Phys.* **79**, 5457 (1983).

²⁹S. Mukamel, *J. Stat. Phys.* **27**, 317 (1982); **30**, 179 (1983); in *Random Walks and Their Applications in the Physical and Biological Sciences*, edited by M. F. Schlesinger and B. J. West (AIP, New York, 1984).

³⁰R. F. Fox, *Phys. Rep.* **48**, 180 (1978).

³¹R. Zwanzig, in *Boulder Lectures in Theoretical Physics*, edited by W. Brittin (Wiley, New York, 1960), Vol. II.

³²We have deleted the spontaneous decay term usually included in Eqs. (3) since it can be removed by a simple transformation of $P(t)$ (see Ref. 14).

³³This method could be generalized by replacing $1/\epsilon$ not by $G_0(\epsilon)$, but by any function $h(\epsilon, c_T, c_D)$ which has a naive expansion similar to Eq. (25).

³⁴J. Nieuwoudt and S. Mukamel, *J. Stat. Phys.* (to be published).

³⁵W. Magnus, F. Oberhettinger, and R. P. Soni, *Formulas and Theorems for the Special Functions of Mathematical Physics* (Springer, New York, 1966), p. 35. See also Refs. 23 and 24.

³⁶Other postulates were also made, e.g., $G_0(t) \sim At^{-\alpha}$, $At^{-\alpha}(\ln t)^\beta$. Both were found to violate the SCE. If the postulate $G_0(t) \sim A \exp(-\beta t^\alpha)$ is made, the SCE is violated unless $\alpha = 1$.

³⁷Other postulates were also made. If $G_0(t) \sim A \exp(-t^\alpha)$ is made, the COP SCE no longer requires that $\alpha = 1$. However, for the rates (i) and (iii), for which exact solutions are found, $\alpha = 1$ and consequently we have set $\alpha = 1$ for exponential rate (ii) also.

³⁸The exact solution is discussed in Sec. VI.

³⁹W. Y. Ching, D. L. Huber, and B. Barnett, *Phys. Rev. B* **17**, 5025 (1978).

- ⁴⁰G. Korzeniewski, R. Friesner, and R. Silbey, *J. Stat. Phys.* **31**, 451 (1983).
- ⁴¹G. Korzeniewski and D. Calef, *J. Phys. C* **16**, 4599 (1983).
- ⁴²E. W. Montroll and G. Weiss, *J. Math. Phys.* **6**, 167 (1975).
- ⁴³M. F. Schlesinger and E. W. Montroll, *Proc. Natl. Acad. Sci.* **81**, 1280 (1984).
- ⁴⁴Y. Gefen, A. Aharony, and S. Alexander, *Phys. Rev. Lett.* **50**, 77 (1983).
- ⁴⁵R. B. Pandey and D. Stauffer, *Phys. Rev. Lett.* **51**, 527 (1983).